sciendo

Slovak Journal of Civil Engineering

Vol. 27, 2019, No. 3, 44 – 54

DOI: 10.2478/sjce-2019-0021

STATIC AND DYNAMIC RESPONSES OF A REINFORCED CONCRETE BEAM STRENGTHENED WITH STEEL AND POLYPROPYLENE FIBERS

Radhika SRIDHAR[1]*, Ravi PRASAD[1]

Abstract

This paper describes an experimental investigation on mono steel and polypropylene (PP) fiber-reinforced concrete beams. The main aim of this present study is to evaluate undamaged and damaged reinforced concrete (RC) beams incorporated with mono fibers such as steel and PP fibers under free-free constraints. In this experimental work, a total of nine RC beams were cast and analyzed in order to study the dynamic behavior as well as the static load behavior of steel fiber-reinforced concrete (SFRCs) and polypropylene fiber-reinforced concrete (PPFRCs). Damage to the SFRC and PPFRC beams was obtained by cracking the concrete for one of the beams in each set under four-point bending tests with different percentage variations of the damage levels such as 50%, 70% and 90% of the maximum ultimate load. The fundamental natural frequency and damping values obtained through the dynamic tests for the SFRC and PPFRC beams were compared with a control RC beam at each level of damage that had been acquired through static tests. The static experimental test results emphasize that the SFRC beam has attained a higher ultimate load compared with the control RC beam.

Address

[1] Dept. of Civil Engineering, National Institute of Technology, Warangal, India

* ***Corresponding author:*** radhikasridhar9@student.nitw.ac.in

Key words

- SFRC,
- PPFRC,
- Damage,
- FRF,
- Damping,
- Four-point test,
- Dynamic,
- Flexure.

1 INTRODUCTION

Concrete is the most commonly used construction material all over the world because of its versatility and availability. Due to the environmental service conditions and complexity of structures such as high-rise buildings, dams, bridges, hydraulic structures, and offshore structures, any normal grade or ordinary concrete can no longer meet general requirements (Soutsos et al., 2012). It is well known, nevertheless, that the correlation between the compressive strength and flexural strength or the split tensile strength of ordinary concrete or high-strength concrete will be inevitably brittle in nature (Habel and Gauvreau, 2008). In order to overcome this drawback, research has focused on various necessary treatments such as adding fibers to concrete, the use of supplementary mineral admixtures, and externally strengthening members with fiber-reinforced polymers (Hao et al., 2016). Amongst these, the addition of fibers like steel, polypropylene, polyvinyl alcohol and natural and synthetic fibers to concrete has been widely accepted because of their improved mechanical properties, i.e., compressive strength, split tensile strength, flexural strength, and flexural toughness (Min et al., 2014). The most commonly used fibers are steel fibers because of their high tensile strength and greater modulus of elasticity. Concrete reinforced with steel fibers has been extensively used in the building industry in applications such as chimneys, industrial buildings and air pavements, reinforcements of projected concrete, and pre-cast or post-tensioned elements (Caverzan et al., 2011). Besides steel fibers, the most extensively used fiber materials in concrete for reinforcement purposes in recent decades have involved inventive solutions obtained by adding non-metallic polypropylene fiber and cementitious materials (Tiberti et al., 2014). They are predominantly mentioned in the manufacture of fiber-reinforced concrete, and their behavior has been especially investigated with the aim of understanding the possible synergetic action of mono

fibers in order to enhance the post-cracking strength or response of a structure. A structure which is reinforced either with steel or PP fiber provides strengthening properties to the same structure (Dawood and Ramli, 2010). Flexural-shear or shear cracks can occur at different stages and sizes in concrete, so the use of various fibers with different aspect ratios are a better way to rectify the problem (Kim et al., 2011). The main purpose of adding fibers of various aspect ratios is to control both micro and macro cracks at different zones of the cementitious material at different damage levels and during different impact loading or dynamic loading conditions (Yang et al., 2011).

In general, concrete structures will always be subjected to vibration forces such as impact loading from the dynamic shock of moving vehicles. Depending on the type of structure and the impact or dynamic load, harmonic excitation exists through the external force of a certain frequency applied to a system for a given amplitude (Barros and Dias, 2006). Damage assessment plays an important role in the evaluation of the stability and strength of a structure, which is significant for both existing structures and those under construction (Huang et al., 2010). In recent decades, structural health monitoring has been used in enormous civil engineering applications such as bridges, frames, towers and beams and also in new vibration research (Zsolt, 2008). The flexibility to assess any concrete structure and perceive damage in its earliest state can be easily done or achieved only through a vibration analysis method (Capozucca, 2011). The essential concept concealed by the vibration monitoring technique for a damage analysis of any RC structures would be based on the dynamic characteristics and does not rely on the geometry of the structure; as a result, changes can occur in the dynamic response behavior (Capozucca, 2013). Besides the vibration-based monitoring technique, numerous methods have been studied by researchers to analyze damage such as changes in the modal strain energy method, the flexible method, and the updated structural model method (Malej et al., 2010). Venglar and Sokol (2017) studied the damage assessment of a simply supported beam numerically through the vibration-based method, which is the most promising non-destructive technique, and concluded that the computation times as well as the desired accuracy of the damage assessment had been improved. The dynamic parameters of steel truss bridges have been studied through ambient vibration measurements that could be used as a comparative basis in the future for repeated measurements (Venglar et al., 2018; Sokol et al., 2015). The main dynamic parameters of structural materials such as mass, stiffness, damping, fundamental frequency, mode shape, and amplitude of excited force could provide the dynamic behavior of any structure.

1.1 Significance of research

Significantly more research is needed that addresses the enormous and various conditions that are inherent in applying the vibration monitoring technique for the assessment of the structural integrity of any RC beams strengthened with fiber-reinforced concrete. Based on the aforementioned approaches, an experimental program has been developed and formulated to evaluate the damage assessment of mono steel and PP fiber-reinforced concrete beams under dynamic tests. The experimental research was developed with large-scale modelling of SFRC and PPFRC beams. A total of nine RC beams were cast by incorporating mono steel and PP fibers and also control RC beams to attain the objective of the present study as well as to compare the SFRC and PPFRC beams with control RC beams.

2 EXPERIMENTAL PROGRAM

A damage assessment of RC beams incorporated with steel and polypropylene fibers was designed and studied under static and dynamic load tests. In order to evaluate the effect of fibers in a damaged and undamaged condition, steel and PP fiber-reinforced concrete composites have been developed and studied individually with the addition of different fiber dosages to the total fiber volume fraction of the concrete accompanied with mechanical property tests such as compressive, split tensile and flexural strength tests. In this experimental investigation, a damage assessment of the SFRCs and PPFRCs was carried out for the optimum steel and PP fiber contents.

Tab. 1 *Physical and mechanical properties of steel and polypropylene fibers*

Fiber type	Shape of fibers	Length (mm)	Diameter (mm)	Aspect ratio	Tensile strength (MPa)	Modulus of elasticity (GPa)	Density (kg/m^3)
Steel	Hooked-end	35	0.5	70	1100	210	7850
PP	Straight	12	0.038	315	420	5	990

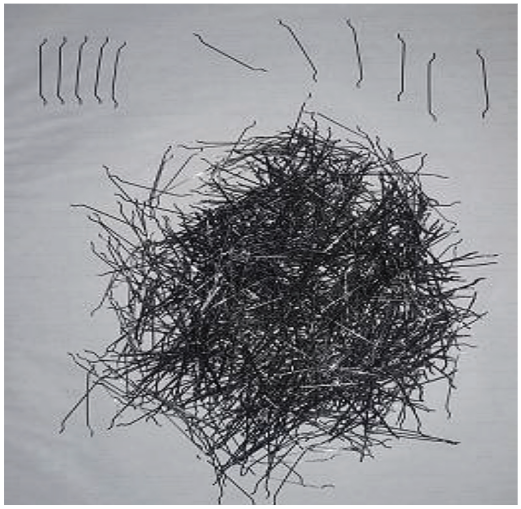

Fig. 1 *Typical view of steel fibers*

Fig. 2 *Typical view of PP fibers*

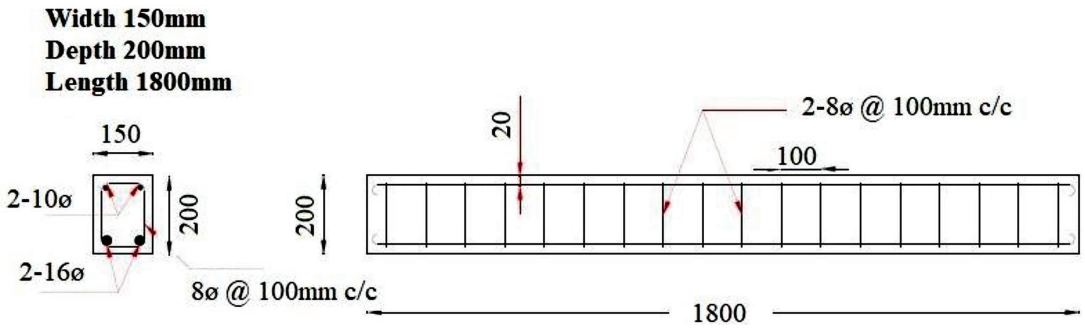

Fig. 3 *Detailing of reinforced concrete beam*

Tab. 2 *Designation of the RC beam specimens*

Mix No	Beam designation	Beam type	Type of test
1	M25Control-S (A_1)	RC	Static
2	M25Control-D (A_2)	RC	Dynamic
3	M25Steel-S (C_1)	SFRC-strengthened	Static
4	M25Steel-D (C_2)	SFRC-strengthened	Dynamic
5	M25Polypropylene-S (E_1)	PPFRC-strengthened	Static
6	M25Polypropylene-D (E_2)	PPFRC-strengthened	Dynamic

2.1 Basic constituents of materials

Ordinary 53 grade Portland cement (OPC) according to the Bureau of the Indian Standard Code was used in this study; it has a specific gravity of 3.15 and a bulk density of 1140 kg/m^3 (IS:12269:2013).

The cement was replaced by fly-ash at approximately 10% of its mass in order to attain the desired strength of M25 grade concrete and also to ease the dispersion of the fibers to the concrete. Coarse aggregates with maximum and minimum sizes of 20 mm and 10 mm with a 6.34 fineness modulus was used. Locally available river sand having a fineness modulus of 2.86 was used as the fine aggregate. Tap water mixed with super-plasticizers was used to mix the ingredients in order to increase the workability of the mixture. The steel and PP fiber-reinforced concrete composites were prepared using different fiber volume fractions with different percentage variations of 0%, 0.5% 0.75%, 1% and 1.25% and 0%, 0.1%, 0.2%, 0.3% and 0.4% of concrete, respectively in this present work; one optimum fiber dosage was chosen for casting each of the SFRC and PPFRC beams in order to evaluate the dynamic behaviours. The steel fibers used in this investigation were hooked-end, whilst the PP fibers were straight. The aspect ratio of the PP and steel fibers used in this study are 315 and 70, respectively. The steel and PP fibers were produced in a locally available market. The physical and mechanical properties of the steel and PP fibers are tabulated in Tab. 1. Figs. 1 and 2 show a typical view of the steel and PP fibers used in this study.

2.2 Fabrication of specimens

In this experimental investigation, a total of nine RC beams were fabricated and cast. Also, ten mixtures of steel and PP fiber-reinforced concrete composites were prepared using different fiber volume fractions of concrete in order to examine the mechanical properties of the SFRCs and PPFRCs.

All the RC beam specimens were initially designed to be 1800 mm long with a rectangular cross-section of 150 mm wide and 200 mm high. All the beams were designed as under-reinforced sections based on the area of tensile reinforcement to prevent the catastrophic failure of the structure. Each beam was reinforced with high-tensile strength bars of Fe500; the detailing of the RC beam is shown in Fig. 3. For each mixture, RC beams were cast and tested to evaluate the ultimate load through a static load test. From the ultimate load obtained, 50%, 70% and 90% of the ultimate loads were achieved and then employed to determine the degree of damage of another set of beams achieved with the same mixture. The designations of the SFRC, PPFRC and control RC beams are illustrated in Tab. 2.

2.3 Mixing, casting and curing procedures

The concrete mix design was prepared according to the Indian Standard Code for Concrete Mix design, which is based on the technical properties of the material (IS:10262:2009). The mixing process started with the dry mixing of the coarse and fine aggregates for one minute. The cement was added and mixed for another minute. Then the steel fibers were added to the mixture, and the mixing was continued for another two minutes till the fibers were dispersed properly through a visual inspection for casting the mono SFRC specimens. Water mixed with super-plasticizers was added and mixed for another 2 minutes.

After the first process was completed, polypropylene fibers were added to the wet concrete, and the mixture was mixed for another 3 minutes to ensure that the fibers were evenly dispersed throughout the concrete for casting the PPFRCs. Then the fresh concrete was cast in steel molds for cubes, cylinders and prisms and was compacted on a vibration table, where a needle vibrator was used for casting the RC beams. All the specimens were demolded after 24 hours and were then immersed in water at a room temperature of 27º C for 28 days. The mix proportion of the control, steel, PP fiber-reinforced composites and RC beams are tabulated in Tab. 3. Fig. 4 displays the casting of the RC beams.

(a) *Steel moulds for casting* the *RC beam*

(b) *Casting of RC beams*

Fig. 4 *Preparation sequences of RC beams*

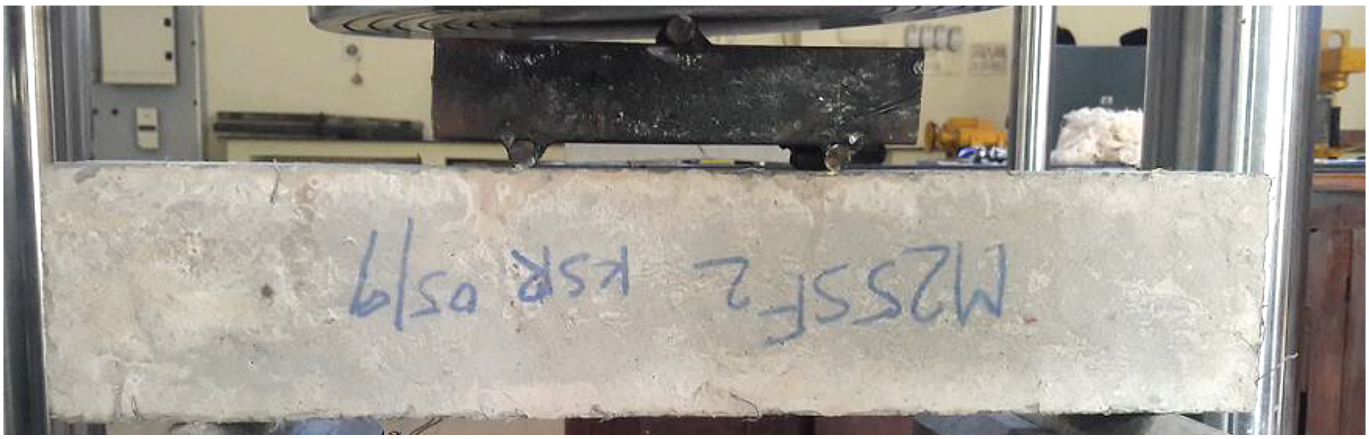

Fig. 5 *Typical view of the flexural test setup*

2.4 Mechanical property tests

To examine the composite performance of the fiber-reinforced concrete such as the steel and PP fibers, three cubes and cylinders of a standard size (150 mm x 150 mm x 150 mm) and (150 mm diameter and 300 mm height) respectively, were cast for each mixture and tested in a Universal Testing Machine (UTM) with a capacity of 3000 kN to evaluate the compressive and split tensile strengths. All the specimens were loaded until complete failure under a load control at a loading rate of 1.30 kN/min after 28 days of its curing period in accordance with the Bureau of Indian Standard Code (IS:516-2004). A four-point bending flexural test was carried out in this investigation to evaluate the composite performance of the plain and fiber-reinforced concrete. A 500 mm x 100 mm x 100 mm beam was used in this study. The mid-span length of 133.33 mm is one-third of the simply supported clear span length of 400 mm, and the support span of the four-point bending test setup is 50 mm. All the specimens were tested with a dynamic universal testing machine with a capacity of

Tab. 3 *Mix proportion of the control, steel, PP fiber-reinforced composites and RC beams*

Mix No	Designation	Cement	Fly-ash	Fine aggregate	Coarse aggregate	W/C ratio	Steel Fiber (%)	PP Fiber (%)
1	M_1	1	0.1	1.89	2.89	0.42	0	0
2	M_{SF1}	1	0.1	1.89	2.89	0.42	0.50	0
3	M_{SF2}	1	0.1	1.89	2.89	0.42	0.75	0
4	M_{SF3}	1	0.1	1.89	2.89	0.42	1.00	0
5	M_{SF4}	1	0.1	1.89	2.89	0.42	1.25	0
6	M_{PP1}	1	0.1	1.89	2.89	0.42	0	0.10
7	M_{PP2}	1	0.1	1.89	2.89	0.42	0	0.20
8	M_{PP3}	1	0.1	1.89	2.89	0.42	0	0.30
9	M_{PP4}	1	0.1	1.89	2.89	0.42	0	0.40
10	A_1 & A_2	1	0.1	1.89	2.89	0.42	0	0
11	C_1 & C_2	1	0.1	1.89	2.89	0.42	1.00	0
12	E_1 & E_2	1	0.1	1.89	2.89	0.42	0	0.30

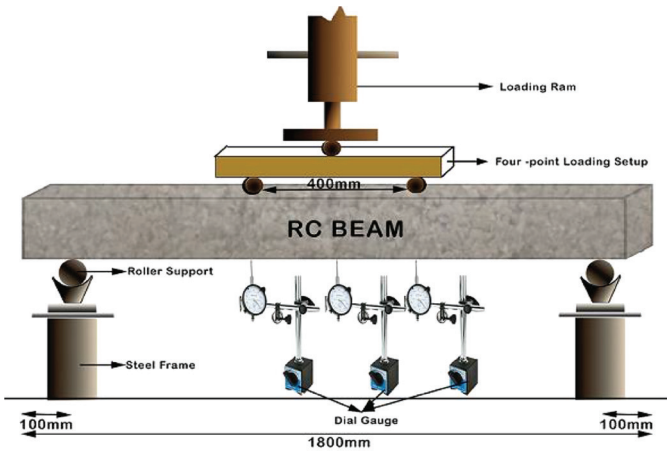

Fig. 6 *Schematic view of the static load test set up*

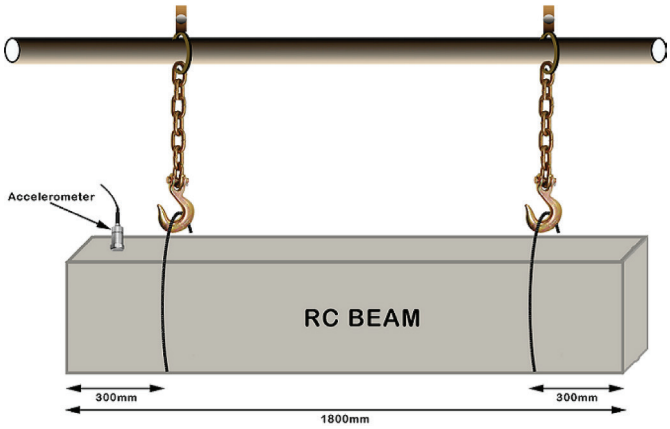

Fig. 7 *Schematic view of beam in free-free constraint*

1000kN, and the specimens were loaded until complete failure under displacement control at a loading rate of 0.20 mm/min. A typical view of the flexural test set up is shown in Fig. 5.

2.5 Static load test procedure of the RC beams

In this experimental investigation, all the beams were tested with the UTM of a 3000kN capacity to evaluate the ultimate flexural load and maximum bending moment of the control RC beams and fiber-reinforced beams (SFRC and PPFRC). An RC beam specimen was placed on a steel support with rollers on each end, and the load was applied through a four-point loading system. Three dial gauges were used to determine the central and overall deflection of the beam at each and every loading point. The schematic view of the static load test setup is shown in Fig. 6.

2.6 Dynamic test procedure

A modal test was performed on both the damaged and undamaged beams using a transfer function technique in free-free constraints. A schematic view of the reinforced concrete beam in free-free constraints is shown in Fig. 7.

It can be clearly seen from Fig. 8, that the accelerometer was placed on the specimen at one particular node to collect the response while vibrating the structure. The modal analysis was carried out using a dynamic analyzer in this study. It consists of an input as well as an output device. The sensitivity of the impulse hammer and accelerometer used in this investigation are (±15%) 0.23 mV/N and (±5%) 1000 mV/g, respectively. As shown in the figure, there is a central unit that receives the signal from the input device and sends it to the computer for further analysis. All the data tested can be stored in the computer and can be retrieved in any form as per the requirements. The Frequency Response Function (FRF) obtained from the dynamic analyzer is fed into a smart office-NV solution to obtain the required output, where a single degree of freedom analysis is carried out in order to get the modal parameters. All the specimens were tested in a free-free condition by keeping the accelerometer at one constant node that was fixed, and the specimens were excited using an impact hammer at any point. The corresponding FRF was recorded at that point in order to evaluate the natural frequency for the damage assessment.

The aforementioned procedure was repeated for all the other 30 points without moving the accelerometer from the initial point; this method is referred to as the roving impact hammer method (Tirelli and Vadillo, 2013). A channel analyzer was used to obtain the signals and the frequency response function (FRF) from the response and the excitation force through the hammer. Fig. 8 depicts the set-up of the modal testing. The modal parameters, such as the natural frequency, damping ratio and mode shape, were extracted through the modal analysis software. Also, the modal test was performed for all the beams at the end of each damage degree as D_0 (undamaged condition), D_1 (50% of the ultimate load), D_2 (70% of the ultimate load) and D_3 (90% of the ultimate load) to examine the dynamic behavior of the control RC, SFRC, and PPFRC beams.

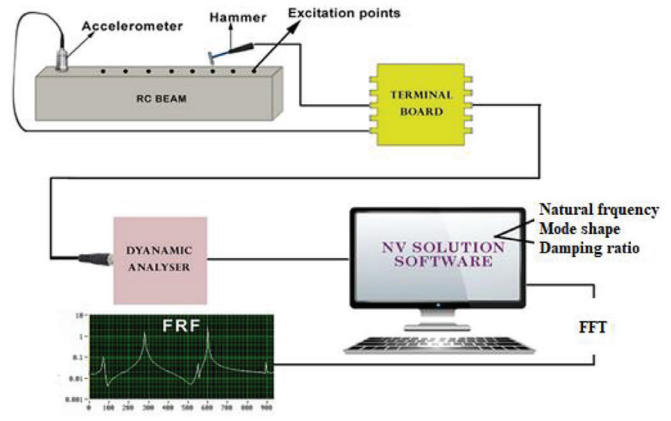

Fig. 8 *Typical view of dynamic test setup*

Tab. 4 *Mechanical property test results of the control, steel and PP fiber reinforced concrete*

Mix No	Designation	Compressive strength (MPa)	Splitting tensile strength (MPa)	Flexural strength (MPa)
1	M_1	34.87	3.39	4.74
2	M_{SF1}	36.34	3.81	5.42
3	M_{SF2}	38.24	4.05	6.04
4	M_{SF3}	39.12	4.53	6.76
5	M_{SF4}	38.45	4.29	6.28
6	M_{PP1}	36.09	3.53	5.02
7	M_{PP2}	36.52	3.84	5.51
8	M_{PP3}	37.70	4.21	6.07
9	M_{PP4}	36.26	3.62	5.39

3 RESULTS AND DISCUSSION

The results acquired through the experimental tests are discussed in this chapter. The static results elucidate the behavior of the control RC, SFRC and PPFRC beams, while the dynamic results show the dynamic response behavior of the aforementioned beams in both damaged and undamaged states under free-free constraints.

3.1 Mechanical properties of the SFRC and PPFRC composites

3.1.1 Compressive strength

Tab. 4 summaries the experimental compressive strength results for the control, SFRC and PPFRC composites. Each magnitude of strength shown in the table is a mean of three specimens tested in the laboratory after the proper curing period. The M_{SF3} mixture, which is incorporated with a 1% total volume fraction of steel fiber, attained the highest compressive strength at the age of 28 days of 39.12 MPa, which was increased by about 12% when compared with the non-fibrous concrete. The results emphasize that the addition of fibers such as steel and PP in terms of the volume fraction of concrete resulted in an inherent increase in compressive strength when compared with the non-fibrous concrete (M_1). The test results also indicate that the compressive strength of the SFRCs and PPFRCs increased with an increase in the total fiber volume fraction. Amongst the different percentage variations of the mono steel and PP fibers considered in this experimental study, the highest compressive strength was achieved for the mixtures containing 1% of steel fiber and 0.3% of PP fiber, which was increased by about 12% and 8%, respectively. Also, these percentages are considered as optimum dosages for casting RC beams strengthened with fibers.

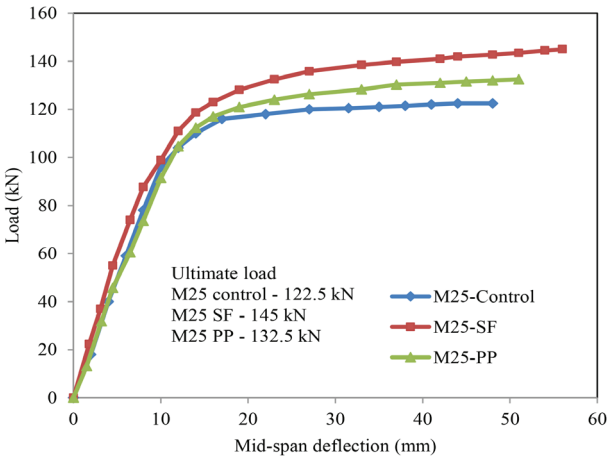

Fig. 9 *Load vs. mid-span deflection of the control and fibre-reinforced concrete beams*

3.1.2 Splitting tensile strength test

The results obtained from the splitting tensile strength test for the control, SFRC and PPFRC are tabulated in Tab. 4. The tensile strength results of the control concrete was decreased about 25% and 19.5% when compared with the highest values attained for the M_{SF3} and M_{PP3} mixtures respectively, because ordinary concrete is known to be ductile in compression and brittle in tension. The results indicate that the addition of fibers exhibited a better performance than that of the non-fibrous concrete composites. The enhancement of the split tensile strength for the M25 grade of concrete with the addition of steel fibers ranged from 12.4% to 33.6% for the M_{SF1} and M_{SF3} mixtures, respectively. In the primary cracking stage of the concrete, there were numerous staple fibers (PP) bridging the micro-cracks and preventing the expansion of the PPFRCs. Whereas, when the tensile

(a) *Control RC beam at damage degree D_2*

(b) *PPFRC beam at damage degree D_3*

Fig. 10 *Failure patterns of RC, SFRC and PPFRC beams at different damage levels*

stress maintained ruined the specimens, the stress was transformed to the steel fibers in the case of the SFRCs, which have a greater Young's modulus and tensile strength.

3.1.3. Flexural strength

Four-point bending tests were accomplished on three specimens for each percentage variation of the concrete mixture to examine the flexural strength of the steel and PP fiber-reinforced composites. The results obtained for the different percentage variations of the SFRCs, PPFRCs, and control concrete are illustrated in Tab. 4. The load versus mid-span displacement was monitored during each test. It can be observed from the table that the flexural strength of the SFRC specimen was increased up to 42.6% for the M_{SF3} composites when compared to the control concrete. The test results distinctly indicate that the presence of high tensile strength steel fiber influences the flexural strength as well as the split tensile strength in different ways. PP fibers are short and have a lower tensile strength and elastic modulus, whereas steel fibers are long and have a higher tensile strength and

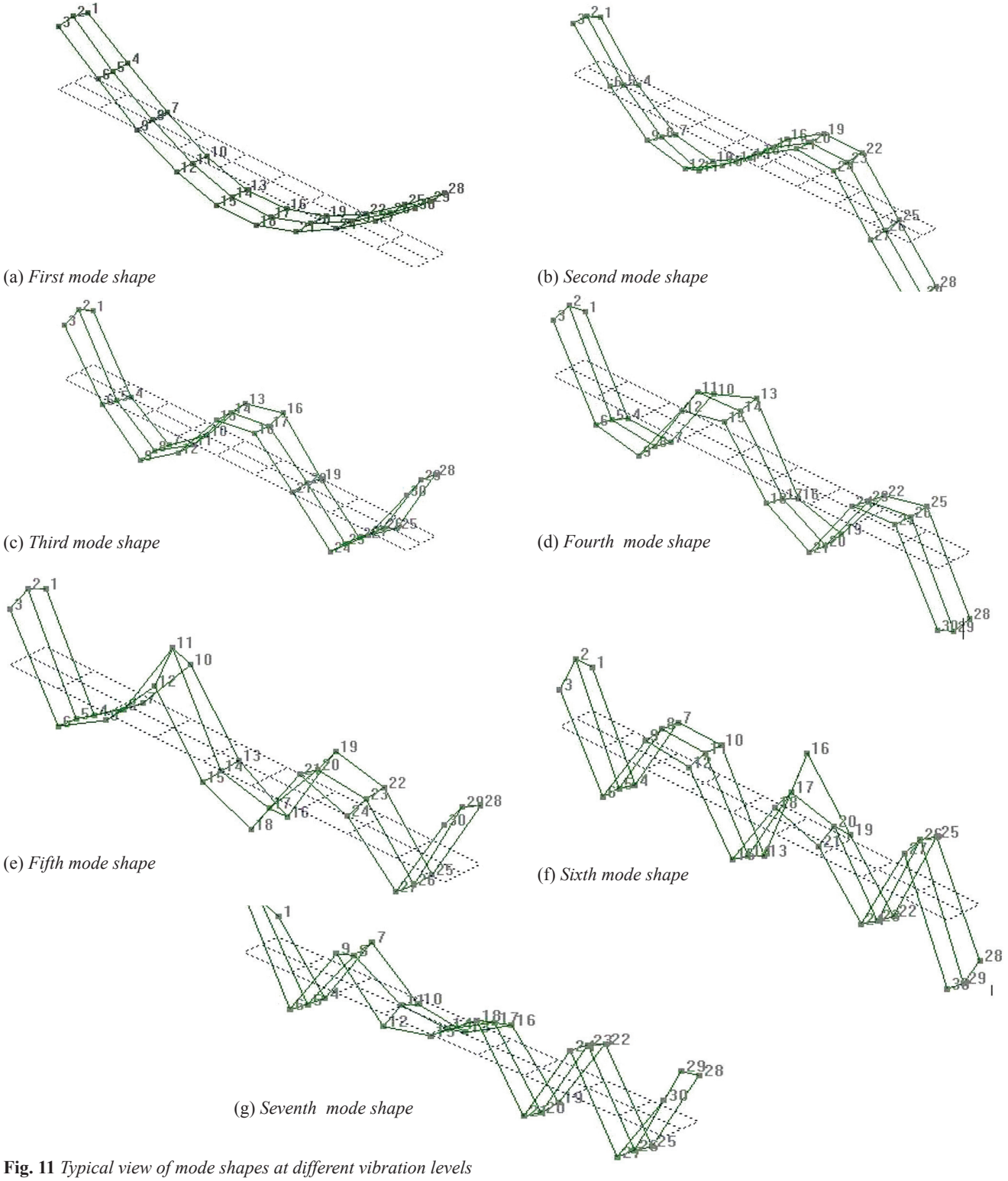

(a) *First mode shape*

(b) *Second mode shape*

(c) *Third mode shape*

(d) *Fourth mode shape*

(e) *Fifth mode shape*

(f) *Sixth mode shape*

(g) *Seventh mode shape*

Fig. 11 *Typical view of mode shapes at different vibration levels*

elastic modulus, which can bridge the micro and macro-cracks of the PPFRCs and SFRCs, respectively, thereby resulting in a significant improvement in flexural strength.

3.2. Static analysis of RC, SFRC and PPFRC beams

Beams A_1, C_1 and E_1 were control RC beams that were subjected to a monotonic bending test to examine the ultimate load and the flexural vibrations in an undamaged state that had also been carried out before the testing. All the RC, SFRC, and PPFRC beams were examined under a complete bending failure for the static analysis; the partially bending loading increased the damage from D_0 to D_3. All the RC beam specimens were subjected to monotonic static loads at two points in the mid-span equal to 400 mm in order to get flexure-shear failure. From the static load test setup, it can be seen that the specimen was instrumented with three dial gauges at mid-point and at the loading points to evaluate the deflection of the beam while testing. All the beams were washed white, and girds were marked on two sides of a 50 mm x 50 mm beam for the purpose of locating the progression of any cracks. Fig. 9 shows the load versus the mid-span deflection behavior of the RC, SFRC and PPFRC beams. It can be seen from the graph that in the elastic region, the load applied was very low and that the deflection of the beam was also less, in accordance with the plane bending assumption theory.

There was an extrinsic decrease in the stiffness of the beam due to the formation of line-hair cracks in the tension zone; the load at this point was 40kN, 54kN, and 49kN for the beams A_1, C_1 and E_1, respectively. When the load increased, cracks propagated on the sides of the beam, which sustained a greater load at a constant stiffness;

Tab. 5 *Natural frequency values of the control RC beam - A_2 (f)*

Damage degree	Load (kN)	f_1 (Hz)	f_2 (Hz)	f_3 (Hz)	f_4 (Hz)	f_5 (Hz)	f_6 (Hz)	f_7 (Hz)
D_0	0	221.3	579.7	1051	1608	2211	2836	3481
D_1	61.25	205.4	534.8	1011	1520	2123.1	2789	3259
D_2	85.75	189.6	509.4	972.3	1436	1935.2	2564	2978
D_3	110.25	172.1	497.1	924.8	1360	1782	2356	2815

Tab. 6 *Damping ratio values of the control RC beam - A_2 (ζ)*

Damage degree	Load (kN)	Mode 1	Mode 2	Mode 3	Mode 4	Mode 5	Mode 6	Mode 7
D_0	0	0.93	0.61	0.57	0.43	0.41	0.37	0.35
D_1	61.25	0.97	0.65	0.59	0.46	0.44	0.39	0.38
D_2	85.75	1.06	0.71	0.62	0.51	0.47	0.43	0.41
D_3	110.25	1.15	0.76	0.65	0.53	0.51	0.46	0.43

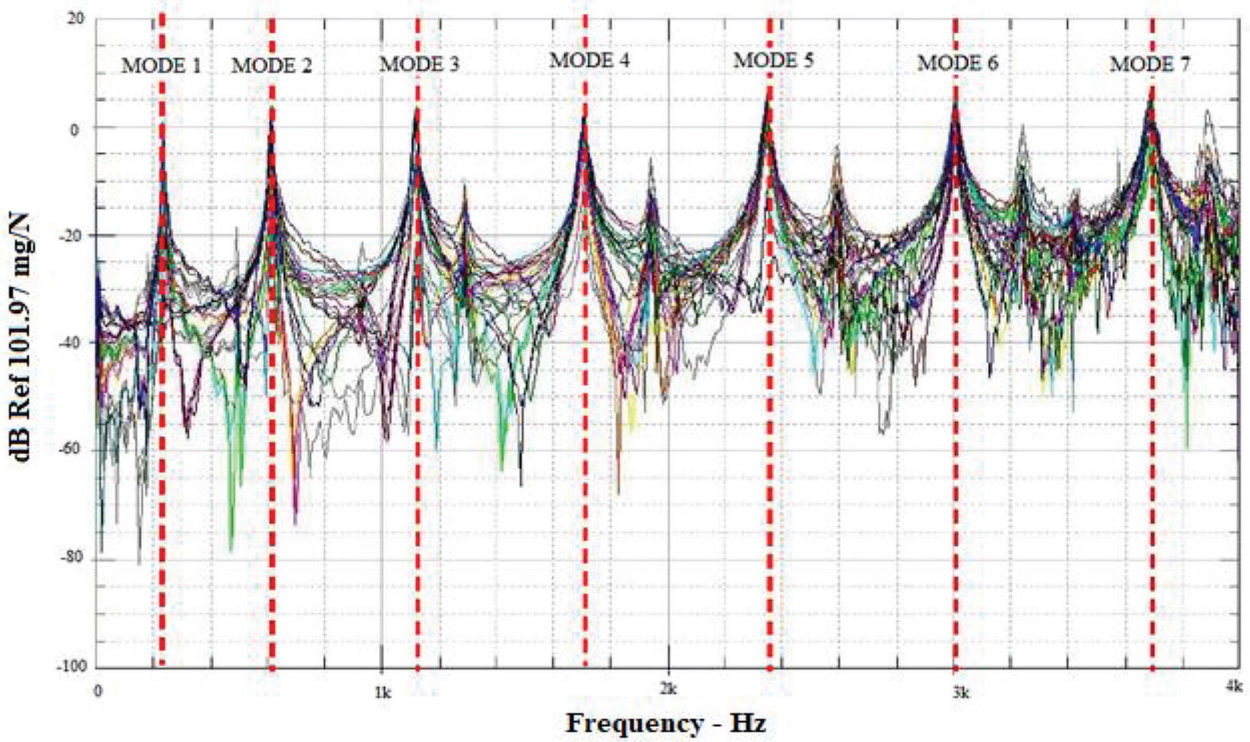

Fig. 12 *Envelope of FRFs in undamaged (D_0) state for the control RC beam*

Tab. 7 *Natural frequency values of the SFRC beam - C_2 (f)*

Damage degree	Load (kN)	f_1 (Hz)	f_2 (Hz)	f_3 (Hz)	f_4 (Hz)	f_5 (Hz)	f_6 (Hz)	f_7 (Hz)
D_0	0	226	583.6	1079	1681	2271	2897	3435
D_1	72.5	212.3	542.4	1000.6	1536	2112	2716	3326
D_2	101.5	201.2	521.2	973	1493	2068	2645	3189
D_3	130.5	196.7	508	955.1	1411	1908	2490	2964

Tab. 8 *Damping ratio values of the SFRC beam - C_2 (ζ)*

Damage degree	Load (kN)	Mode 1	Mode 2	Mode 3	Mode 4	Mode 5	Mode 6	Mode 7
D_0	0	1.03	0.61	0.59	0.53	0.43	0.39	0.35
D_1	72.5	1.04	0.63	0.62	0.55	0.46	0.42	0.37
D_2	101.5	1.07	0.66	0.63	0.56	0.48	0.45	0.38
D_3	130.5	1.1	0.69	0.67	0.59	0.51	0.46	0.41

more cracks progressed towards the tension zone; and hairline cracks were formed in the compression zone under the load points.

Cracks were initiated exclusively in the tension zone with the increase in the loading towards the neutral axis, and the cracks widened and propagated for the control RC beams. Furthermore, the cracked portion was effective in resisting the bending stress and bending moment; the load-carrying capacity coincided with the yielding of the steel. Eventually, the crack enlarged more in the tension zone than in the compression zone after the complete yielding of the reinforcement. Fig. 10 shows the failure patterns of the control RC, SFRC and PPFRC beams under the monotonic loading condition. Beams A_1, C_1 and E_1 failed in flexure at the ultimate loads of 122.5kN, 145kN and 132.5kN with maximum deflections of 48 mm, 56 mm and 52 mm, respectively.

3.3 Flexural vibration analysis of the RC, SFRC and PPFRC beams

The A_2, C_2 and E_2 beams were analyzed by dynamic tests to measure the dynamic characteristics at different states of the damaged as well as the undamaged conditions. Dynamic tests were conducted for all the beams through such non-destructive methods as the impact hammer technique at the end of each degree of damage as D_1, D_2 and D_3 in free-free constraints. Dynamic parameters such as the natural frequency, damping ratio, FRF and mode shapes were obtained for all the specimens through experimental flexural vibration tests. Generally, the form of the FRFs used in the experimental technique is inertance, which returns a measure of the amplitude in terms of acceleration, starting from random excitations through the Fast Fourier Transform (FFT) method (Wang et al., 2016). The experimental natural frequency and damping ratio values of the control RC beam (A_2) are illustrated in Tabs. 5 and 6, respectively. The aforementioned beam was analyzed by a dynamic test at the undamaged level (D_0), which was followed by static and dynamic tests at the end of each damage level from D_1, D_2 and D_3 as 50%, 70% and 90% of the ultimate load, respectively, which was taken from beam A_1. From the dynamic results obtained, the natural frequency decreased with increases in the damage, whereas the damping ratio increased with increases in the structural damage of the beam. Fig. 11 arbitrarily displays the mode shapes of the reinforced concrete beams. The envelope of the frequency response functions (FRFs) are shown in Fig. 12 for the control RC beam in an undamaged state, which was obtained by a dynamic test in the frequency range of 0-4000Hz.

Tab. 9 *Natural frequency values of the PPFRC beam - E_2 (f)*

Damage degree	Load (kN)	f_1 (Hz)	f_2 (Hz)	f_3 (Hz)	f_4 (Hz)	f_5 (Hz)	f_6 (Hz)	f_7 (Hz)
D_0	0	228.4	590.8	1043	1615	2225	2845	3481
D_1	66	216.5	562.8	1009	1597	2107	2684	3323
D_2	92.4	199.1	536.9	988	1512	2038	2567	3219
D_3	118.8	186.4	514.4	970	1427	1968	2476	3116

Tab. 10 *Damping ratio values of the PPFRC beam - E_2 (ζ)*

Damage degree	Load (kN)	Mode 1	Mode 2	Mode 3	Mode 4	Mode 5	Mode 6	Mode 7
D_0	0	0.97	0.56	0.49	0.45	0.43	0.41	0.36
D_1	66	0.99	0.59	0.52	0.47	0.44	0.44	0.38
D_2	92.4	1.02	0.61	0.54	0.48	0.47	0.45	0.40
D_3	118.8	1.05	0.64	0.57	0.51	0.49	0.47	0.43

A similar dynamic response technique was used to analyze the SFRC and PPFRC beams (C_2 and E_2) at each damage level. The natural frequency and damping ratio values for the SFRC beam are tabulated in Tabs. 7 and 8, respectively. Moreover, the natural frequency and damping ratio values for the PPFRC beam are tabulated in Tabs. 9 and 10, respectively. The percentage decrease in the natural frequency at every damage level decreased for the fiber-reinforced concrete beams when compared with the control RC beams. It can be observed from the experimental results that the damping values increased with the increase in the degrees of damage. The percentage increase in the damping ratio at every damage level decreased for the fiber-reinforced concrete when compared with the control RC beams.

4 CONCLUSION

In this experimental investigation, the static and dynamic behavior of fiber-reinforced concrete was studied and compared with control RC beams. The following conclusions have been drawn from the experimental results:

1. The fiber-reinforced concrete mixtures resulted in enhanced behavior in terms of the overall performance of the static properties accompanied by compressive, splitting tensile and flexural strengths when compared with the control concrete.

2. The flexural strength increased with the addition of both the steel and PP fibers individually when compared to the control concrete; it also enhanced the post-cracking behavior of the concrete. The flexural strength of the steel fiber-reinforced concrete was increased by about 42.6% when compared with the non-fibrous concrete.

3. The gain in the splitting tensile strength was improved, depending upon the addition of the total volume fraction of mono fibers in the concrete. The increase in the concrete's splitting tensile strength at the age of 28 days for the total volume fraction of the 1% steel fiber was about 33.6%, which is greater than the PP fiber-reinforced concrete composites as well as the control concrete.

4. In the static test of the SFRC and PPFRC beams, the addition of fibers that were incorporated either with steel or PP fibers led to an increase of about 18.36% and 8.1% for the C_1 and E_1 beams, respectively, when compared with the control RC beams.

5. From an undamaged state to the damage degree D_3, the natural frequencies for both the control RC beam and fibrous-reinforced concrete beams decreased with the increase in the damage's intensity, whereas the damping ratio increased with an increase in the damage's intensity.

6. Finally, the vibration-based monitoring technique is one of the best methods used to assess damage of reinforced concrete beams and could also be correlated to the loading degrees. Changes from the uncracked to the cracked sections were recorded by decreasing the natural frequency values.

REFERENCES

Soutsos, M. N. - Le T. T. – Lampropoulos, A. P. (2012) *Flexural performance of fibre reinforced concrete made with steel and synthetic fibres*. Construction and building materials, Vol. 36, pp. 704–710.

Habel, K. – Gauvreau, P. (2008) *Response of ultra-high performance fiber reinforced concrete (UHPFRC) to impact and static loading.* Cement and Concrete Composites, Vol. 30, pp. 938-946.

Hao, Y. – Hao, H. – Chen, G. (2016) *Experimental investigation of the behaviour of spiral steel fibre reinforced concrete beams subjected to drop-weight impact load.* Materials and Structures, Vol. 49, pp. 353-370.

Min, K. H. – Kwon, K. Y. – Lee, J. Y. – Yoon, Y. S. (2014) *Effects of steel fibre and shear reinforcement on static and impact load resistances of concrete beams*. Magazine of Concrete Research, Vol. 66, pp. 998-1006.

Caverzan, A. – Cadoni, E. – Prisco, M. D. (2011) *Dynamic tensile behavior of self-compacting steel fiber reinforced concrete*. Applied Mechanics and Materials, Vol. 82, pp. 220-225.

Tiberti, G. – Minelli, F. – Plizzari, G. A. – Vecchio, F. J. (2014) *Influence of concrete strength on crack development of SFRC members.* Cement and Concrete Composites, Vol. 45, pp. 176-185.

Dawood, E. T. – Ramli, M. (2010) *Development of high strength flowable mortar with hybrid fiber*. Construction and Building Materials, Vol. 6, pp. 1043-1050.

Kim, D.J. – Park, S. H. – Ryu, G. S. – Koh, K. T. (2011) *Comparative flexural behavior of hybrid ultra-high performance FRC with different micro fibers*, Construction and Building Materials, Vol. 25(11), pp. 4144-4155.

Yang, K. H. (2011) *Tests on concrete reinforced with hybrid or monolithic steel and polyvinyl alcohol fibers*, ACI Materials Journal, Vol. 108(6), pp. 664-672.

Barros, J. A. O. – Dias, S. J. E. (2006) *Near surface mounted CFRP laminates for shear strengthening of concrete beams*. Cement and Concrete Composites, Vol. 28(3), pp. 276-292.

Huang, X. – Ma, G. W. – Li, J. C. (2010) *Damage assessment of reinforced concrete structural elements subjected to blast load.* International Journal of Protective Structure, Vol. 1(1), pp. 103-124.

Zsolt, H. (2008) *Vibrations of cracked reinforced and pre-stressed concrete beams*. Archives of Civil and Mechanical Engineers, Vol. 6(2), pp. 155-164.

Capozucca, R. (2011) *Damage assessment of PRC and RC beams by dynamic tests*. Journal of Physics Conference Series, Vol. 305(1).

Capozucca, R. (2013) *A reflection on the application of vibration tests for the assessment of cracking in PRC/RC beams.* Engineering Structures, Vol. 48, pp. 508-518.

Maalej, M. – Chhoa, C. Y. – Quek, S. T. (2010) *Effect of cracking, corrosion and repair on the frequency of RC beams*. Construction and Building Materials, Vol. 24, pp. 719-731.

Venglar, M. – Sokol, M. (2017) Choice of appropriate control values for effective analyses of damage detection. Slovak Journal of Civil Engineering, Vol. 25(1), pp. 24-28. DOI: 10.1515/scje-2017-0004.

Venglar, M. – Sokol, M. – Aroch, R. (2018) Ambient vibration measurements of steel truss bridges. Slovak Journal of Civil Engineering, Vol. 6(4), pp. 234-239. DOI: https://doi.org/10.21595/jme.2018.20419.

Sokol, M. – Venglar, M. – Sokol, M. – Aroch, R. – Fabry, M. (2015) Damage detection of a bridge. Proceedings of the 6th International Conference on Mechanics and Materials Design, Portugal, pp. 247-254.

Tirelli, D. – Vadillo. I. (2013) A fast automated impact hammer test method for modal parameter extraction implementation on a composite bridge beam. Non-destructive Testing of Materials and Structures, Springer, pp. 999-1006. DOI: 10.1007/978-94-007-0723-8_140.

Wang, L. – Lie, S. T. – Zhang. Y. (2016) Damage detection using shift path. Mechanical Systems and Signal Processing, pp. 298-313. DOI: 10.1016/j.ymssp.2015.06.028.

IS 12269:2013, Ordinary Portland cement 53g – specification.

IS 10262:2009, Guidelines for concrete mix proportioning.

IS: 516-2004, Indian standard methods of tests for strength of concrete.